ORIGINAL ARTICLE

Effect of nano-conversion on morphological, rheological and thermal properties of barley starch

Suman Kumari[1] · Baljeet S. Yadav[1] · Ritika B. Yadav[1]

Abstract The aim of the present study was to synthesize biodegradable starch nanoparticles (SNP's) from a renewable source like barley starch and to characterize for morphological, crystalline, thermal, and rheological properties. Acid hydrolysis transformed A+V-type round or disc-shaped native starch (NS) granules with an average width of 10 μm and the average length of 22 μm into round or irregular shaped A-type SNP's with an average size of 64 nm with the crystallinity enhanced from 41.75 to 48.08%. The zeta potential of NS and SNP's was − 17.7 and − 21.4 nm, respectively, with the higher stability of SNP's. The gelatinization temperature increased while melting decreased after nano conversion of barley starch. The storage and loss moduli of 12 and 15% suspension of SNP's remained unchanged with a change in angular frequency (0.1–10 rad-s), which indicated a greater tendency to recover after deformation, while 20% SNP's suspension behaved like a viscous fluid. The flow behavior test demonstrated a shear-thinning behavior of SNP's suspension.

Keywords Barley starch · Nanoparticles · Morphology · Rheological properties · Thermal properties

✉ Baljeet S. Yadav
  baljeetsingh.y@gmail.com

  Suman Kumari
  skumari0211@gmail.com

  Ritika B. Yadav
  rita.by@rediffmail.com

[1] Department of Food Technology, Maharshi Dayanand University, Rohtak, Haryana, India

Introduction

In recent years, increasing interest in nanotechnology, especially in bio-nano materials, has led to various researches in the area of nano-sized particles of natural origin. Nanoparticles are solid particles ranging from 1 to 100 nm in size, which may be organic, inorganic, or surface modified. Previous studies have shown that various organic and edible nanoparticles can be prepared from food-based ingredients, such as polysaccharides, lipids, proteins, etc. (McClements 2014). Starch is one of the most promising polysaccharides for nanoparticle fabrication because of its biodegradable nature, non-toxicity, low cost, ease of production, and cyclic availability. The amylose component of starch is a linear molecule linked by α (1–4) glycosidic bonds, whereas amylopectin is a multiple branched molecule and the backbone chains (composed of 10–60 glucose units) of amylopectin are linked by α (1–4) glucosidic bonds (around 95%) and side chains (made up of 15–45 glucose units) are linked by α (1–6) bonds (around 5%), branching points are localized every 22–70 glucose units and responsible for the crystallinity.

Starch nanoparticles are crystalline portions derived from the disruption of amorphous regions of starch granules by acid hydrolysis. Starch nanoparticles have many benefits over native starch owing to their extremely small size and larger surface area with minimum diffusion limitation. SNP's have exhibited diverse applications in emulsion stabilization (Ge et al. 2017), biodegradable composites (Xu et al. 2018), encapsulation (Ahmada et al. 2019), etc.

The botanical sources of starch, as well as preparation methods, have been reported to influence the morphological and other functional characteristics of the SNP's (Xu et al. 2018). Various preparation methods of SNP's such as

acid hydrolysis, enzymatic hydrolysis, precipitation, gamma irradiation; mechanical methods such as reactive extrusion and high-pressure homogenization have been reported to influence the morphological and crystalline characteristics of SNP's as spherical shaped SNP's have been produced by adopting self-assembly of short glucan chains (Liu et al. 2016), while square-like platelet-shaped nanoparticles have been synthesized via acid hydrolysis (Mukurumbira et al. 2017). Further, the size, shape, concentration, and distribution of nanoparticles in the suspension are also known to affect the pasting and rheological properties of the starch nano-suspensions (Song et al. 2008).

Barley (*Hordeum Vulgare L.*) is one of the first crops to get domesticated and cultivated commercially worldwide. The barley grain occupies about 60–70% starch as the main component (Kong et al. 2016). The industrial use of barley is mainly limited to malt preparation. Therefore, the systematic information on the morphological, crystalline, thermal, and rheological properties of barley starch-based SNP's could be useful to diversify the application profile of barley for food as well as non-food applications. Thus, the objective of the present study was to prepare barley SNP's and to characterize them for their morphological/microstructural, crystalline, thermal, and rheological properties to assess their suitability for industrial applications.

Materials and methods

Isolation and preparation of barley SNP's

Barley grains of a standard variety (BH-393) purchased from Haryana Agricultural University, Hisar (India) were used for the isolation of starch using the method as suggested by Subaric et al. (2011). *The isolated starch was analyzed for its chemical composition and amylose content.* Barley SNP's were prepared by acid hydrolysis (10.0 g dry starch/100 ml of 3.16 M sulphuric acid, 37 °C for 7 days, stirring rate 100 rpm) of the native starch as suggested by Angellier et al. (2005) with some minor modification.

Microscopic studies

The size and shape of barley NS and the SNP's were analyzed by light microscopy. The phenomenon of birefringence was studied using polarized light microscopy (Olympus CX 21 i Led). Morphological properties of NS and SNP's were studied using SEM at 3.00 KX and 100.00 KX magnifications for NS and SNP's respectively (Zeiss EVO 50). For NS, the sample was sprinkled whereas; SNP's were suspended in ethanol to prepare 0.1% suspension and one drop of the suspension was applied on

double-sided carbon tape, dried and coated with gold–palladium and examined under SEM. TEM of SNP's was performed using TEM (JEOL-JEM-1400 electron microscope, Japan) with an acceleration voltage of 120 kV. A drop of ethanolic suspension (100%, w/v) of SNP's sonicated for 10 min was deposited on the carbon-coated copper grid, dried and examined under TEM.

Particle size distribution and zeta potential

Particle size analysis of NS was performed in particle size analyzer (Mastersizer 3000, Malvern UK) using a laser light scattering technique equipped with a hydro-dispersion unit. Distilled water was used as a dispersant and wet dispersion method was adopted for measurement. The sample was poured in the sample cell up to the obscuration limit was reached to 15–20% following ultrasonic dispersion. The size distribution was recorded as a function of diameters Dv(10), Dv(50), and Dv(90) which indicate 10, 50 and 90% of the total volume of starch particles.

The average particle size and polydispersity index (PDI) of SNP's were determined at 25 °C using a Zetasizer (Malvern Instruments Ltd., Zetasizer version, 7.11, Malvern, UK). For sample preparation, the SNP's were dispersed in ethanol to obtain a 0.1% (w/v) suspension followed by sonication for 10 min to remove the aggregation of particles and filtration through syringe filter of size 2.45 μm to remove microparticles. Immediately after filtration, the sample was used for the measurement of average particle size (Z-average size) and PDI, and Zeta potential was recorded with a Nano Zetasizer (Malvern, UK).

XRD analysis

Degree of crystallinity was determined by X-ray diffractometer (X'pert PRO on PAN analytical diffractometer) using a copper anode X-ray tube equipped with Cu-Kα (1.54 A°) radiation and with exposure of the sample to the X-ray beam at 45 kV and 40 mA with a diffraction angle (2θ) ranging from 4 to 40° with a step 0.02°. A smooth curve was computer plotted on diffractograms.

Pasting properties

Rapid Visco-analyser (RVA Starch master™, Newport Scientific, Australia) was used for studying the pasting properties of the samples. A programmed heating and cooling cycle of the starch dispersion (3.0 g starch/25 ml water) started with the equilibration of the sample at 50 °C for 1 min, heating to 95 °C in 4 min and 30 s, holding for 2 min and 30 s followed by cooling to 50 °C in 4 min and further holding at the same temperature for 1 min. The

starch suspension was stirred at 960 rpm for the initial 10 s and then at 160 rpm for the remainder of the test. The peak viscosity (PV), hot paste viscosity (HPV), cold paste viscosity (CPV), pasting temperature, breakdown viscosity (BD = PV-HPV), and setback viscosity (SB = CPV-HPV) and peak time (P_{time}) were measured.

Rheological properties

For rheological properties, native starch gels with varying concentrations of 6, 8, and 10% were prepared and cooled at room temperature before studying the amplitude sweep, frequency sweep, and flow behavior. However, no gelling properties were obtained in case of SNP's at the same concentrations since acid hydrolyzed the amorphous regions. So, higher concentrations of SNP's suspensions (12, 15, and 20% (w/v) were used for this purpose.

Continuous shear rate or flow behavior

The test was performed at 25 °C with a shear rate range of $0.1–100$ s^{-1} to determine the relationship between shear stress and a shear rate of SNP's. The experimental data were fitted to the Herschel Bulkley model equation as given below:

$$\tau = \sigma \cdot (Pa) + K\gamma^n$$

where, τ represent the shear stress (Pa), σ = yield stress, γ is the shear rate (s^{-1}), n is flow behavior index (dimensionless), K is consistency coefficient (Pa.s^n).

Dynamic rheological properties

Dynamic rheological tests were performed with a dynamic rheometer (MCR 102, Anton Paar, Germany) having a parallel plate (40 mm diameter, 1 mm gap) geometry using 1 ml of gel/suspension sample. The sample was allowed to equilibrate for 2 min before each measurement.

The frequency sweep test was performed at room temperature (25 °C) with an angular frequency ranging from 0.1 to 10 rad/s at 1% (NS gel) and 10% (SNP's suspension) strain values. The change in storage modulus (G′), loss modulus (G″), and loss tangent (tan δ = G″/G′) with angular frequency (0.1–10 rad/s) was recorded. The temperature sweep test was performed at a strain of 10% and heating rate of 5 °C/min from 25 to 90 °C.

Thermal properties

6.0 mg sample was added with 3.0 μl of deionized water into an aluminum pan of the DSC instrument (Q-10, TA Instrument Waters). The pan was hermetically sealed and thermally scanned over a temperature range of 25–150 °C at a heating rate of 10 °C/min. The empty aluminum pan was taken as a reference and to avoid the condensation during scanning the sample chamber was flushed with dry nitrogen. The onset temperature (T_0), peak temperature (T_p), conclusion temperature (T_c), and gelatinization enthalpy were analyzed.

Statistical analysis

Analysis of variance was performed by one way ANOVA followed by Tukeys HSD test ($p < 0.05$) using SPSS version 19.0. The results were interpreted as the mean of three independent determinants.

Results and discussion

The isolated barley NS was of high purity with a protein content of only 0.32%. The total amylose content and apparent amylose content of the isolated starch were 18.73% and 15.95%, respectively. Amylose content is considered as an important component impacting the overall properties of the starch as well as the preparation of SNP's.

Microscopic characteristics

The microscopic structures of NS and SNP's as studied by simple light and plane-polarized light microscopy are shown in Fig. 1. Barley NS had mostly round-shaped granules with some oval shaped granules with a smooth surface under light microscopy (Fig. 1a). The polarized light micrographs as shown in Fig. 1b, revealed that no birefringence was observed in case of a SNP's and a mixture of irregular and round-shaped particles were observed, possibly because of the loss of arranged order of crystalline and amorphous regions (Fig. 1c, d).

The SEM as illustrated in Fig. (1e and f) showed disc-like or round or oval shaped NS granules with an average width of 10 μm and an average length of 22 μm and with plane outer surface. In contrast, SNP's were observed as round and irregular shaped particles aggregates with an average size of 64 nm. The formation of aggregates of nanoparticles could be attributed to the hydrogen bond formation due to the presence of hydroxyl groups on the outer surface of nanoparticles. The SEM studies of the SNP's have reported irregular or platelet like (Sivamani et al. 2018), which suggested that shape and size of SNP's depends not only on the starch source but also on the preparation methods. Some food-grade acids like citric acid also have a significant influence on the morphology of starch. A loss in the smooth surface of starch has been noticed in citric acid hydrolyzed (5% acid, at 45 °C, for

Fig. 1 Simple Light microgram (40X) of barley NS (**a**); polarized light microgram of native starch (40X) (**b**); Simple light microgram of SNP's at 10X (**c**); at 40X (**d**); SEM of NS (3000x) (**e**); SNP's (10000x) (**f**); TEM of SNP's (50000x) (**g**)
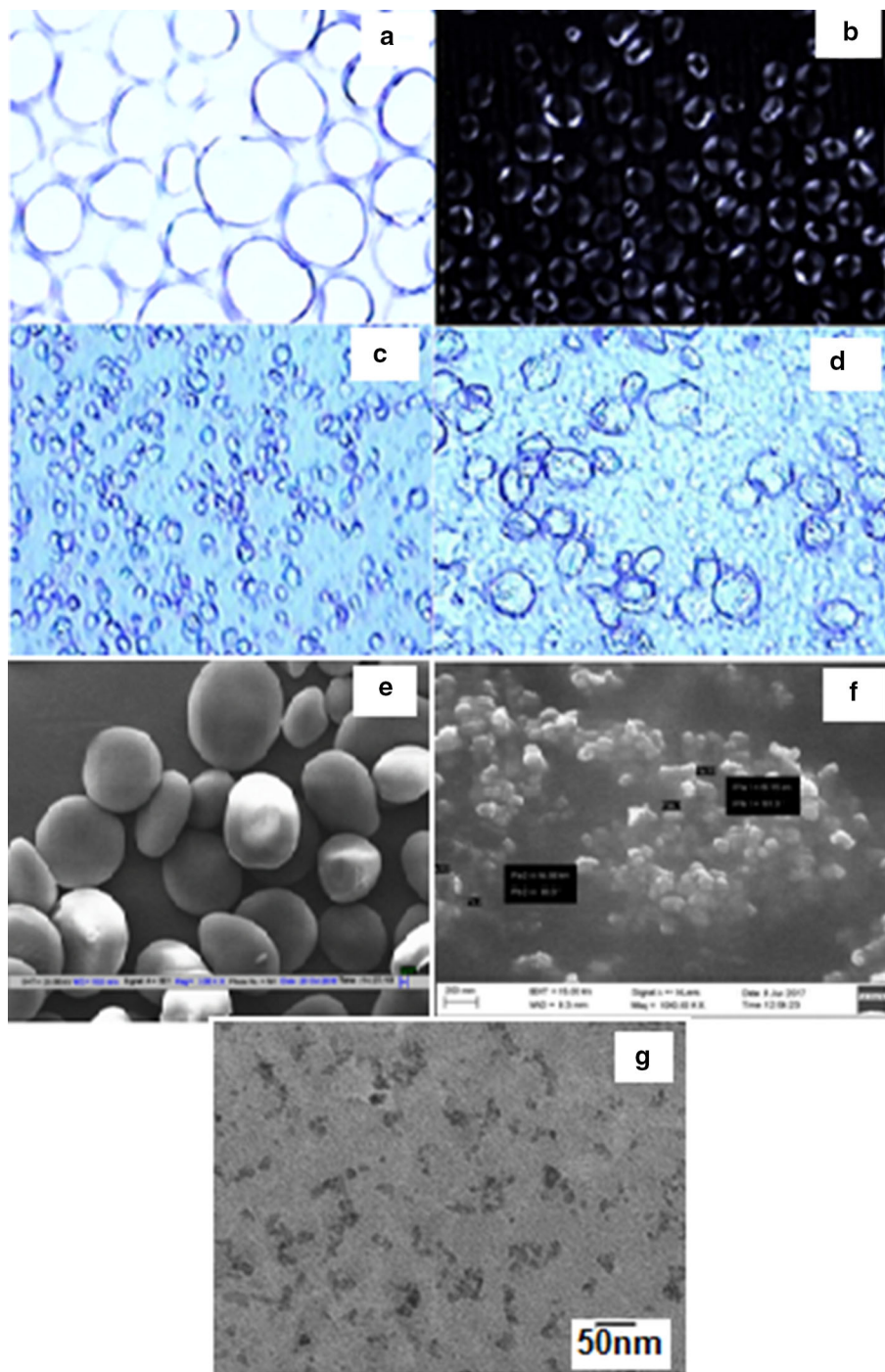
11 h) sweet potato starch. It was attributed to the acid erosion to the core part of the granules. On the other hand, there was no reduction/change in the size of starch granules obtained from citric acid hydrolysis. The granule size of native and hydrolyzed starch was 8.61–8.66 μm, respectively, and the size of modified starch granules is greater than the size required for fat replacer (Surendra Babu et al. 2015). Zambelli et al. (2018) reported that the morphology of lactic, acetic, and citric acid (10% solution w/v)

modified cassava starch was not altered by acid modification and was similar to their native counterpart. Hence, in contrast to food-grade acids, sulfuric acid hydrolysis is more proficient in modifying the starch granules' morphology and particle size.

The TEM micrograph of SNP's also showed round or irregular shaped particles with an average size of less than 50 nm with some aggregations (Fig. 1g). There has been suggested a relationship between the size of native starch

granules and the corresponding nanoparticles, smaller the native starch, smaller the corresponding nanoparticles (Qin et al. 2016). Particles size of starches is an important factor in determining the texture of food products. Native and modified starches have been used as a fat replacer and fat mimetic in fatty foods, and it reduced more than 50% fat from the product. Starch imitates some of the physical and organoleptic properties of fat (Babu et al. 2018). Therefore, in the light of this fact barley SNP's could potentially be used as fat replacers owing to the very small size and may replace the high-calorie fat with low-calorie carbohydrates.

Particles size distribution and zeta potential

The NS granules showed a bimodal size distribution curve with size ranging from 0.6 to 45 μm, and size distribution at D(10), D(50), and D(90) was 13.0, 20.1, and 28.8 μm respectively (10, 50, and 90% particles finer than this size). Dynamic light scattering (DLS) was used for the determination of the hydrodynamic diameter of SNP's. The average hydrodynamic diameter of SNP's was recorded to be 140 nm with a PDI value of 0.18. PDI, in relation to particle size distribution, is described as the ratio of the standard deviation (σ) of the particle diameter distribution and the mean particle diameter. PDI is used to estimate the average uniformity of the particles in a solution. The lower value of PDI obtained in the present study was an indicator of the homogenous distribution of narrow sized particles in the colloidal system. Expectedly, SNP's size as measured by SEM and TEM was smaller than the hydrodynamic diameter, which was on account of swelling of SNP's in water and the generation of an electric double layer due to surface charge and inter particles repulsion in the aqueous suspension around the nanoparticles (Boluk et al. 2011).

The zeta potential of SNP's was higher than NS (− 21.4 mV vs. − 17.7 mV). The higher zeta potential of SNP's indicated higher stability of the acid hydrolyzed barley starch over its native counterpart. Values of zeta potential within the ranges ± 20 mV to ± 30 mV suggest weak stability, whereas the values beyond − 30 mV or + 30 mV indicate higher repulsing forces and decreased van der wall's forces between particles rendering high stability to the particles in the dispersion (Bhattacharjee 2016). As studied previously, maize starch nanocrystals also exhibited a negative zeta potential of − 6.7 mV (Wei et al. 2014).

X-ray diffraction studies

The crystallinity of NS and SNP's was investigated by using XRD, and the diffractograms are shown in Fig. 2a. NS exhibited characteristics of A-type crystalline structure with diffraction peaks at Bragg angles (2θ) of 15°, 17°, 18°, 20°, and 23°. The crystalline pattern of SNP's markedly changed to A-type with higher diffraction intensities, which indicated an enhanced crystallinity after nano-size reduction. Percent crystallinity of NS and SNP's was 41.75 and 48.08%, respectively, as acid preferential attacks on amorphous regions during the early stage of acid hydrolysis, thus increasing relative crystallinity; besides, the crystalline region also hydrolyzed very slowly simultaneously with amorphous regions (Le Corre et al. 2010). Increased crystallinity has also been reported previously for cassava peel SNP's prepared with acid hydrolysis (Sivamani et al. 2018).

Pasting properties

The pasting profiles of NS starch and its nanoparticles measured by RVA are illustrated in Fig. 2b, c. The granular native starch was cold water insoluble whereas in contrast, a completely different pasting curve was observed for the SNP's and the viscosity of SNP's dispersion almost remained unchanged during the heating cycle, which indicated that nanoparticles possibly got dissolved in water at a temperature far below the gelatinization temperature of native barley starch, and thus the pasting temperature of SNP's remained undetected under the given conditions. Based upon these observations, it can be suggested that barley SNP's could be incorporated in a liquid system in a concentration even higher than used in this study without much affecting the viscosity and consistency of the system. Exhibition of a low viscosity even at high solid content of starch nanoparticles could find useful industrial applications in liquid foods or in the systems where higher viscosity of the native starch gel is not required. A decrease in peak viscosity, pasting temperature, hot paste viscosity, and cold paste viscosity was observed in a study conducted by Kaur et al. (2007) in wheat starch treated with aqueous hydrochloric acid. Thus, SNP's in comparison to traditional cooked cationic or anionic starches, exhibit low viscosities of their suspensions even at a very high solid concentration, which could be due to the excessive disintegration of starch granules during acid hydrolysis, and partial or complete destruction of the crystalline structure as evidenced in XRD pattern. It has also been hypothesized that starch with a high level of short chains has improved cold storage stability as a high level of short chains would result in a reduced tendency of retrogradation (Sang et al. 2008).

Fig. 2 X-ray diffraction pattern
(**a**); Pasting profiles of NS
(**b**) and SNP's (**c**)
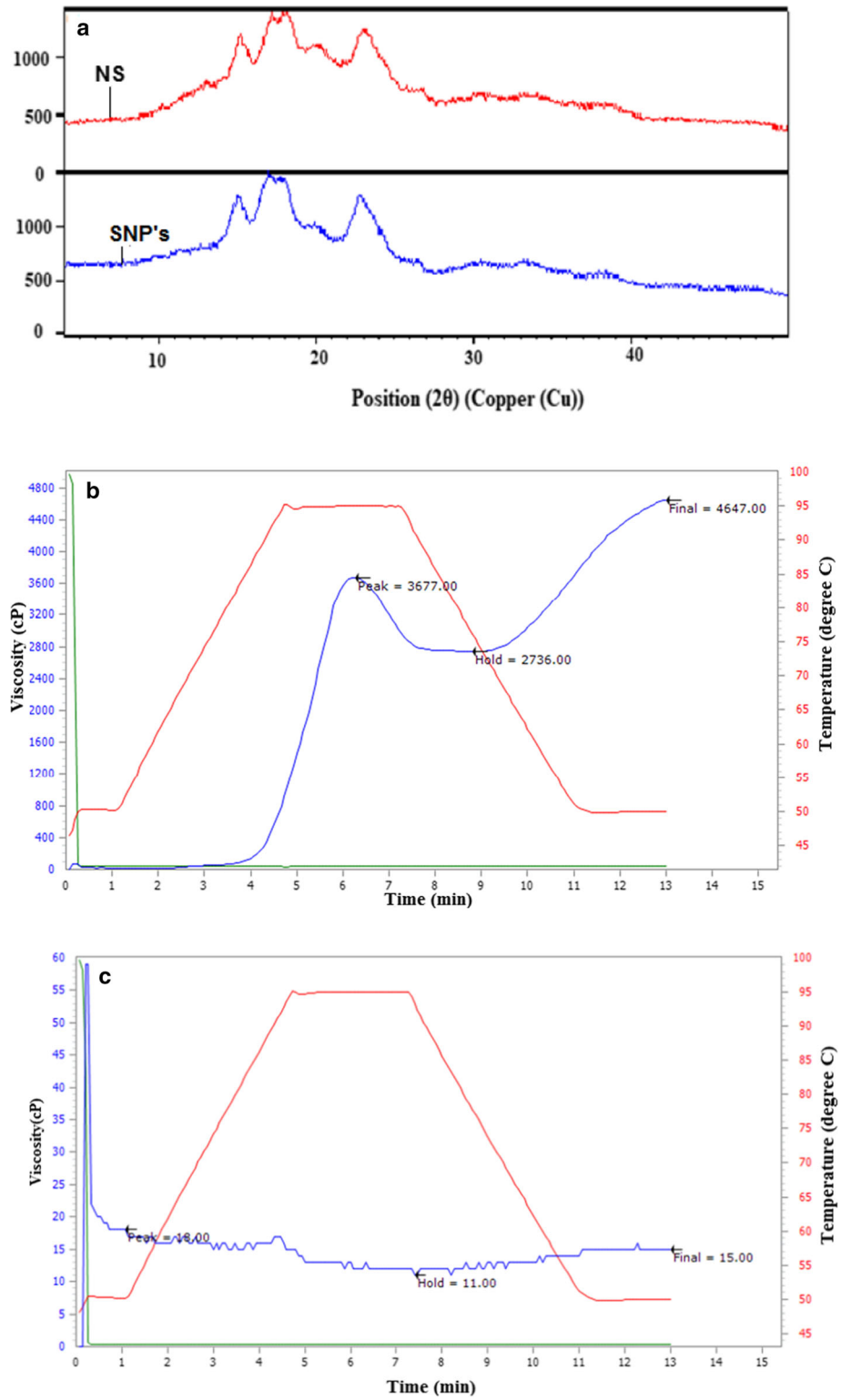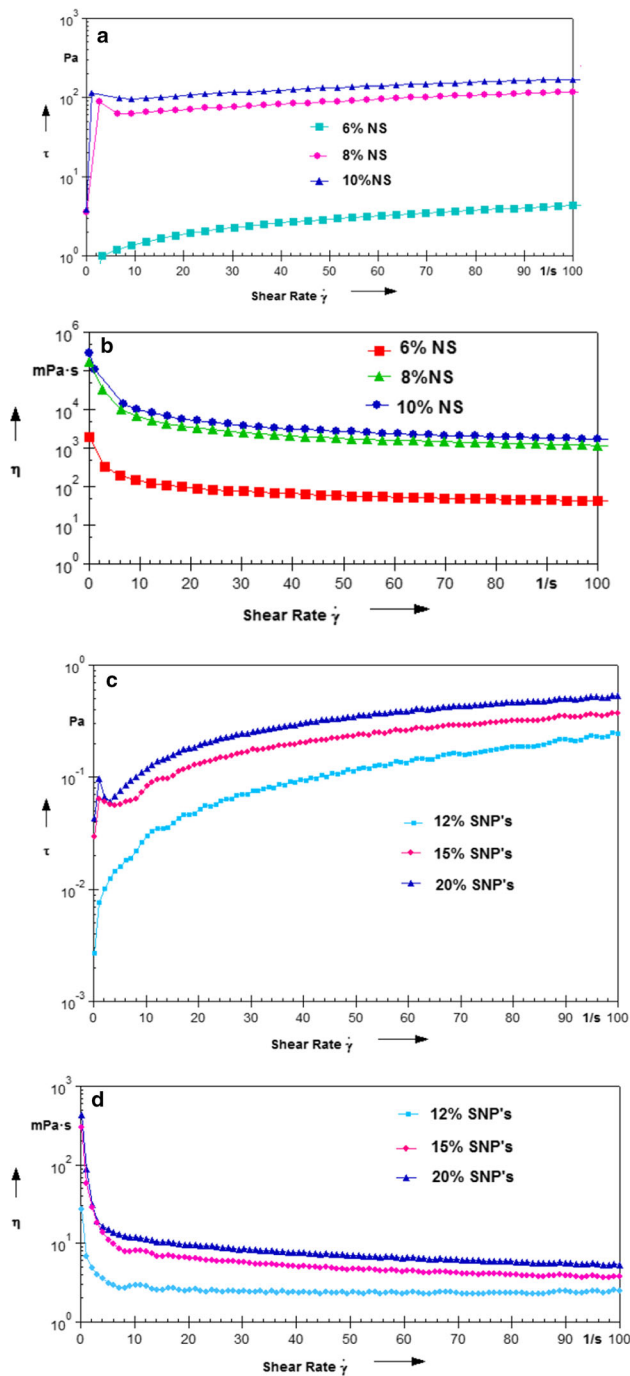
Fig. 3 Flow behavior of NS dispersions at 6, 8, and 10% (w/v) (**a**); viscosity of NS dispersions at 6, 8, and 10% (w/v) (**b**); flow of SNP's dispersions at 12, 15, and 20% (w/v) (**c**); viscosity of SNP's dispersions at 12, 15, and 20% (w/v) (**d**)

Rheological properties

Flow behavior

The flow curves of NS and SNP's, as shown in Fig. 3a and b, showed the relationship between shear rate and shear stress examined at different concentrations. The flow behavior of all the samples was characterized within a shear rate range from 0.1 to 100 s^{-1}. It was observed that the values of shear stress increased with increasing shear rates, and the magnitude of shear stress enlarged as the concentration of starch/nanoparticles increased in the sample. All samples displayed a shear-thinning behavior, belonging to the category of non-Newtonian fluids. NS, as well as SNP's revealed the typical characteristics of pseudoplastic fluids, as evident from Fig. 3a. This decrease in viscosity with increasing shear rates could be attributed to the fact that particles started aligning in the direction of flow under the influence of shear (Fig. 3b).

The flow behavior was assessed using the Herschel-Bulkley model, and the values of various parameters are as given in Table 1. Generally, the values of 'n' decreased with increasing concentration, while an increase was observed in the values of 'K' and yield stress. This could be explained by the fact that higher the concentrations, higher were the particle-particles interactions resulting into higher viscosities. The consistency coefficient (K) values decreased significantly ($p < 0.05$) after nano conversion of micro-sized granules. The yield stress was observed for both barley NS gel and SNP's suspensions, which indicated that to set up the flow, the presence of some cross-linked or interdependent structures in the sample was required to be broken down to initiate the flow of materials.

The values of 'n' were observed to be less than 1 for all samples indicating a pseudoplastic behavior. However, the values of 'n' for NS were lower than SNP's, reflecting that acid hydrolysis caused remarkable changes in the flow properties of starch, and a decrease in the pseudo-plasticity was observed for SNP's. SNP's at lower concentrations, e.g., 12 and 15%, showed a Newtonian and near Newtonian behavior, respectively, while at a higher concentration of 20%, a pseudoplastic behavior was observed probably due to the aggregations among nanoparticles (Fig. 3c, d). The liquid-like behavior of SNP's at lower concentrations might be due to the surface charge and repulsive electrical double layer of the nanoparticles. During sulfuric acid hydrolysis of starch, the sulfate esters might have imparted the negative surface charge on the surface of SNP's. The primary changes in viscosity due to surface charged particles occurred due to the electrostatic repulsion within an electrical double layer of fluid and particle, and later the effect was due to the overlapping of double layers between two particles (Rubio-Hernandez et al. 2004). Shear-thinning behavior also has been reported for citric acid hydrolyzed sweet potato starch (5% acid, at 45 °C for 11 h) with $n = 0.22$ at 10% (w/v) concentration (Surendra Babu et al. 2015). Similarly, a pseudoplastic shear thinning behavior has been reported for acetic, lactic, and citric acid (15% w/v) modified cassava starches with increasing shear

Table 1 Flow behavior of NS and SNP's at different concentration

|		Herschel Bulkley model		
Samples	n	K(Pa.s^n)	R^2	σ° (Pa)
SNP's 12%	1.01 ± 0.01[d]	0.0042 ± 0.00[a]	0.9798	0.014 ± 0.00[a]
SNP's 15%	0.83 ± 0.24[c]	0.0084 ± 0.00[b]	0.99434	0.029 ± 0.00[b]
SNP's 20%	0.76 ± 0.01[c]	0.0156 ± 0.00[c]	0.99054	0.037 ± 0.00[c]
NS 6%	0.57 ± 0.01[b]	0.30 ± 0.007[d]	0.99186	0.120 ± 0.01[d]
NS 8%	0.31 ± 0.01[a]	28.08 ± 1.06[e]	0.96309	88.530 ± 1.43[e]
NS 10%	0.27 ± 0.00[a]	50.27 ± 0.34[f]	0.95911	114.97 ± 0.63[f]

NS—Native starch, SNP's—Starch nanoparticles, The values represent the mean ± standard deviation of three independent determinations. [a–f] mean values followed by the same superscript in the same column are not significantly different ($p < 0.05$), on the basis of tukey HSD test. K= Consistency coefficient (Pa s^n); n = Flow behavior index; σ = Yield stress; R^2 = Regression Coefficient

rate (0.1–350 s^{-1}) (Zambelli et al. 2018). In contrast, increased viscosity has been previously reported for 7% cellulose nanocrystals with increasing ionic strength (Shafiei et al. 2014). However, all suspensions exhibit a shear thinning behavior with a decrease in viscosity with increasing shear rate, and the viscosity decreased from 110 to 5.57 mPa.s, 295 to 3.72 mPa.s, and 429 to 5.31 mPa.s for 12, 15, and 20% SNP's, respectively and suggested that low viscosity of SNP's at higher concentrations could be advantageous for industrial use. Generally, low viscosity is desirable in fruit juices and beverages. The SNP's have been used for encapsulation of polyphenols, vitamins, and pigments. Hence, due to the low viscosity of SNP's, even at higher concentrations, these could be incorporated into a different type of liquid foods without much affecting the viscosity of products.

Frequency sweep and temperature sweep

The dynamic mechanical spectra of NS and SNP's compared and demonstrated in Fig. 4. The frequency sweep test is carried out to distinguish the viscoelastic behavior of materials which discover the dependence of storage modulus (G′) and loss modulus (G″) and tan δ procured during the dynamic mechanical testing imply the elastic property, viscous property and physical state of the material, respectively. The G′ evaluates the stored energy in the sample during the deformation cycle while the G″ evaluates the energy depleted per deformation cycle and tan δ is the ratio of two moduli (G″/G′).

The frequency sweep curves of native starch gel determined at three different concentrations, as shown in Fig. 4a, illustrating the typical pattern of starch gels comprising both elastic and viscous characteristics, and no crossover was obtained between G′ and G″ over the entire frequency range. The frequency sweep spectra revealed that the values of storage modulus (G′) were higher than loss modulus (G″) throughout the measured frequencies,
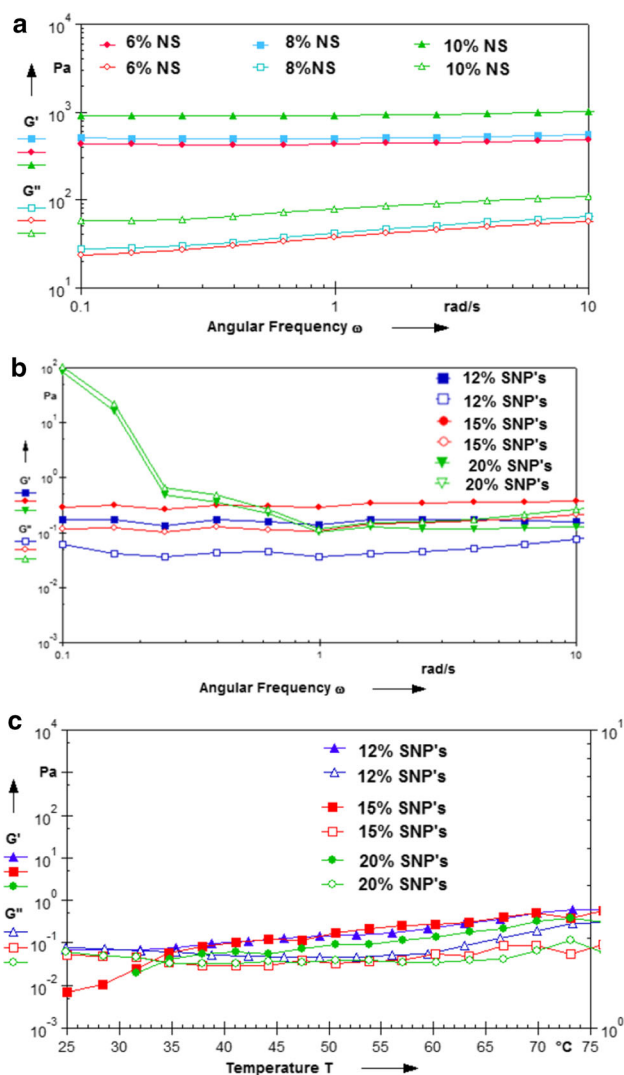
Fig. 4 Frequency sweep curves of NS at 6, 8, and 10% (**a**); Frequency sweep curves of SNP's at 12, 15, and 20% (**b**); temperature sweep curves of SNP's at 12, 15, and 20% (**c**) (storage modulus G′, closed symbol; loss modulus G″, open symbol)

indicating the predominance of elastic behavior over viscous behavior. Further, the G′ of 6, 8, and 10% starch gel was almost constant throughout the frequency range and was independent of the frequency, indicating that no structural changes occurred in the gels, while G″ had shown frequency dependency and decreased at lower frequencies ranges in all studied concentration. Tan δ (G″/G′) is also used to describe the viscoelastic behavior of starch gels, and the values of tan δ were observed to be less than 1 depicting the viscoelastic nature of native barley starch gels having dominated elastic nature. This could be attributed to the intermolecular associations of the amylose chains after leaching, resulting in increased elastic behavior. Due to the thriving requirement of SNP's in food and non-food applications, knowledge of how processing conditions amend the particulate nature and concentration effect of SNP's is of significant interest. The values of G′ and G″ of SNP's suspension exhibited a positive correlation with concentration. It is very clear from Fig. 4b no crossover occurred between G′ and G″ in all samples irrespective of the concentration over the entire frequency range. The frequency sweep spectra revealed that irrespective of the concentration, the values of storage modulus (G′) were higher than loss modulus (G″) throughout the measured frequencies, indicating the predominance of elastic behavior over viscous behavior for 12% and 15% SNP's suspensions. Further, the G′ and G″ of 12% and 15% starch suspension was constant throughout the frequency range and was independent of the frequency indicating that no structural changes occurred in the samples, and these results are consistent with finding of Herrera et al. (2017) potato (49–155 nm) SNP's, while in 20% SNP's suspension both G′ and G″ were dependent on frequency, particularly in the lower frequency range where drastic structural changes occurred and a sharp increase in G′ and G″ was noticed at a lower frequency (below 1.0 rad/s) and had shown viscous behavior was dominated over elastic behavior throughout the frequency range. The finding of the frequency sweep test suggested that barley SNP's could be used up to 15% concentration without altering the texture of food materials since these have elastic nature while beyond 15% concentration give rise to viscous nature. The values of tan δ were less than 1 throughout the frequency range, revealing an elastic behavior in 12 and 15% SNP's suspension while tan δ was greater than 1 for 20% suspension, indicating viscous behavior.

To explain how temperature affects the aqueous nanoparticles network, the viscoelastic behavior of SNP's at a different concentration as a function of increasing temperature were carried out and rheogram of all samples is illustrated in Fig. 4c, which showed the change in storage modulus (G′) and loss modulus (G″) of an aqueous suspension of SNP's. All suspension had shown noticeable cross over point (G′ = G″); at 28 °C for 12%, at 33 °C for 15%, and at 35 °C for 20% SNP's; cross over point symbolic of gel formation with an increase in temperature. Initially, at 25 °C, all suspension behaved like a viscous liquid (G″ > G′), which turned to elastic gel (G′ > G″) with increasing temperature with higher values of storage modulus (G″) than loss modulus (G′). The increase in elastic nature with an increase in temperature in all samples notably observed since heating causes the swelling and melting of SNP's resulting in an increase in viscosity, which can be elaborated by the fact that heating causes disruption of inter and intramolecular bonds in SNP's and subsequent increase in starch water hydrogen bonding (Shi et al. 2013). Shi et al. (2013) reported that the increase in viscosity was might be due to the greater hydrodynamic size of the swelled SNP's. Furthermore, the pattern of change in G″ was similar for all concentrations of SNP's, and it decreased initially and then increased as the temperature elevated. A similar trend of G″ was also reported by Shi et al. (2013) for vacuum freeze-dried potato SNP's added with different concentrations of sodium chloride. In contrast, in a study conducted by Herrera et al. (2017), a decrease (below 70 °C) and then an increase in G′ (above 70 °C) was observed in wheat SNP's, which corresponds to swelling and melting. This transition is associated with the phase transition behavior of native starches as decisive (determined) by differential scanning calorimetry. B-type starches have higher onset temperature, conclusion temperature, and enthalpy of gelatinization than A-type starches; for example, elastic behavior (25–95 °C) was reported in B-type potato SNP's (Herrera et al. 2017). Significant temperature dependency of elastic and viscous nature was observed among all SNP's concentrations.

Thermal properties

The thermal transition behavior of NS and their nanoparticles prepared by sulfuric acid hydrolysis as studied over a temperature range from 25 to 150 °C is as shown in Table 2. Significant differences ($p < 0.05$) were observed among gelatinization temperature and enthalpy of NS and SNP's. Acid hydrolysis significantly influenced the melting temperature as well as enthalpy of barley starch. The onset temperature, peak, and conclusion temperatures of acid hydrolyzed starch were higher than the native counterpart. The gelatinization temperature of 62.37 °C for NS starch increased to 135.87 for barley SNP's. Further, the wider gelatinization temperature range as displayed by NS (58.37 to 69.23 °C) decreased to a narrow extent (135.41–140.30 °C) after the nano conversion of granules via acid hydrolysis. Similar results of increased melting temperatures and broad crystallites melting range for SNP's has been reported by Kim et al. (2013) and Le Corre

Table 2 Thermal properties of NS and SNP's

Samples	Peaks	Transition temperatures (°C)			R (°C) (T$_c$–T$_o$)	ΔH (J/g)	PHI (ΔH/T$_p$–T$_o$)
		T$_o$	T$_p$	T$_c$			
NS	1st	58.76 ± 0.34[a]	62.74 ± 0.37[a]	69.72 ± 0.43[a]	10.95 ± 0.08[b]	6.95 ± 0.11[b]	1.74 ± 0.03[a]
	2nd	109.81 ± 0.24[b]	124.50 ± 0.44[b]	142.48 ± 0.39[b]	32.67 ± 0.15[c]	1241.3 ± 6.61[c]	84.51 ± 1.47[c]
SNP's	1st	135.16 ± 0.32[c]	135.95 ± 0.15[c]	140.55 ± 0.34[b]	4.83 ± 0.20[a]	3.77 ± 0.16[a]	7.97 ± 0.50[b]

NS-Native starch, SNP's-Starch nanoparticles, To, Tp and Tc indicates onset, peak and conclusion temperatures of gelatinization, R- Gelatinization range (Tc–To), ΔH-Enthalpy of gelatinization, PHI-Peak hight index (ΔH/Tp–To). The values represent the mean ±standard deviation of three independent determinations. [a–c] mean values followed by the different superscript in the same column are significantly different ($p <$ 0.05), on the basis of tukey HSD test

et al. (2012) while assessing the influence of botanical origin, amylose content, and crystallinity of starches and the temperature of acid hydrolysis on the thermal properties of starch nanocrystals. This increase in melting temperature after acid hydrolysis might be due to the erosion of preferentially amorphous regions yielding compact crystalline structures necessitating higher thermal energy for the disruption of amylopectin double helices (Kim et al. 2013). The melting enthalpy value of 6.86 J/g for NS starch decreased to 3.60 J/g after acid hydrolysis, witnessing a decrease of about 47% percent. The endothermic enthalpy emulates the crystalline regions, the amount of double-helical of materials, and alters the amylopectin contents and chain length distribution (Ding et al. 2016) and decrease in enthalpy may be due to a change in amylopectin chain length distribution or decrease in compactness of crystals structure of SNP's after nano conversion of barley starch. These observations of higher melting temperature and narrow gelatinization range suggested that some sort of structural rearrangement had been there in the SNP's, as detected by the XRD, crystalline type changed from VA-type for NS to A-type for SNP's. The short chains produced during acid hydrolysis and the annealing before the gelatinization temperature could have induced the structural reorganization. In contrast increase in melting enthalpy after acid hydrolysis reported by Kim et al (2013), which might be due to the erosion of preferentially amorphous regions yielding compact crystalline structures necessitating higher thermal energy for the disruption of amylopectin double helices.

Further, two endothermic peaks were observed only for barley NS. The first peak corresponds to the absorption of water by amorphous growth rings and subsequent disruption of semi-crystalline lamellae causing unpacking of the double helices, and further second peak corresponds to the second melting of the residual crystallites at a higher temperature when water becomes insufficient to swell the starch granules (Le Corre et al.

2012). For dry native starch (corresponding to the second peak), the maximum of the endothermic peak was about 142 °C, which was in the range as observed by Le Corre et al. (2012) for various dry starches. Although this maximum was lower than the normal estimated value of 160–210 °C for the melting of perfect crystallites and this could be possible due to residual moisture content of the NS, which could act as a plasticizer. Based on the results of thermal transitions, it can be concluded that SNP's can be used in wet processes up to nearly a temperature of 140 °C in comparison to about 70 °C for NS. On the basis of the thermal properties of nano-sized particles, the SNP's could be used to enhance the thermal stability of bio-nano composites, which is highly required.

Conclusion

In the present study, round or irregular shaped SNP's were obtained from barley starch by acid hydrolysis at 37 °C with an average diameter of 64 nm. Based on the morphological characteristics of barley SNP's could be used for the reinforcement of the bio-nano composites to improve their barrier properties like water vapor permeability and oxygen permeability. Based upon the results of pasting properties, it can be concluded that barley SNP's could be used in liquid foods at a higher concentration without causing any significant change in viscosity of liquid foods, especially where the high viscosity of the native starch gel is not required. On the basis of the shear-thinning behavior of SNP's, it can be concluded that lower viscosity at higher concentrations could be valuable for industrial applications for SNP's. DSC results revealed that gelatinization temperature was higher for SNP's in comparison to native counterparts, and this attribute could be used to enhance the thermal stability of bio-nano composites. This research represents a basic contribution to the food industry

by demonstrating possible applications of SNP's as texture improver and in bio-degradable films.

Compliance with ethical standards

Conflict of interest The authors declare no conflict of interest.

References

Ahmada M, Mudgil P, Gani A, Hamed F, Masoodi FA, Maqsood S (2019) Nano-encapsulation of catechin in SNP's: characterization, release behavior and bioactivity retention during simulated in-vitro digestion. Food Chem 270:95–104

Angellier H, Dufresne A, Molina-Boisseau S, Lebrun L (2005) Processing and structural properties of waxy maize starch nanocrystals reinforced natural rubber. Macromolecules 3:3783–3793

Babu AS, Parimalavalli R, Mohan RJ (2018) Effect of modified starch from sweet potato as a fat replacer on the quality of reduced fat ice creams. J Food Meas Charact 12:2426–2434

Bhattacharjee S (2016) DLS and zeta potential – what they are and what they are not? J Control Release 235:337–351

Boluk Y, Lahiji R, Zhao L, McDermotto MT (2011) Suspension viscosities and shape parameters of cellulose nanocrystals (CNC). Colloid Surf A Physicochem Eng Asp 377:297–303

Ding Y, Kan J (2016) Characterization of nanoscale retrograded starch prepared by a sonochemical method. Starch - Stärke 68(3–4):264–273

Ge S, Xiong L, Li M, Liu J, Yang J, Chang R, Liang C, Sun Q (2017) Characterizations of Pickering emulsions stabilized by SNP's: influence of starch variety and particle size. Food Chem 234:339–347

Herrera MP, Vasanthan T, Chen L (2017) Rheology of SNP's as influenced by particle size, concentration and temperature. Food Hydrocoll 66:237–245

Kaur R, Gill BS, Sogi DS (2007) Studies on the effect of aqueous hydrochloric acid on properties of wheat starch. J Food sci Technol 44:386–390

Kim HY, Park DJ, Kim JY, Lim ST (2013) Preparation of crystalline starch nanoparticles using cold acid hydrolysis and ultrasonication. Carbohydr Polym 98:295–301

Kong X, Kasapis S, Zhu P, Sui Z, Bao J, Corke H, (2016) Physicochemical and structural characteristics of starches from Chinese hull-less barley cultivars. Inter J Food Sci Technol 51(2):509–518

Le-Corre D, Bras J, Dufresne A (2010) Starch nanoparticles: a review. Biomacromol 11:1139–1153

LeCorre D, Bras J, Dufresne A (2012) Influence of native starch properties on starch nanocrystals thermal properties. Carbohydr Polym 87:658–666

Liu C, Qin Y, Li X, Sun Q, Xiong L, Liu Z (2016) Preparation and characterization of starch nanoparticles via self–assembly at moderate temperature. Int J Biol Macromol 84:354–360

McClements DJ (2014) Nanoparticle and microparticle-based delivery systems: encapsulation, protection, and release of active components. CRC Press, Boca Raton, FL

Mukurumbira A, Mariano M, Dufresne A, Mellem JJ, Amonsou EO (2017) Microstructure, thermal properties and crysatllinity of amadube starch nanocrystals. Int J Biol Macromol 102:241–247

Qin Y, Liu CZ, Jiang SS, Xiong L, Sun QJ (2016) Characterization of SNP's prepared by nanoprecipitation: influence of amylose content and starch type. Ind Crop Prod 87:182–190

Rubio-Hernandez FJ, Carrique F, Ruiz-Reina E (2004) The primary electroviscous effect in colloidal suspensions. Adv Colloid Interface Sci 107:51–60

Sang Y, Bean S, Seib PA, Pedersen J, Shi Y (2008) Structure and functional properties of sorghum starches differing in amylose content. J Agric Food Chem 56:6680–6685

Shafiei S, Hamad WY, Hatzikiriakos SG (2014) Ionic strength effects on the microstructure and shear rheology of cellulose nanocrystal suspensions. Cellulose 21:3347–3359

Shi AM, Wang LJ, Li D, Adhikari B (2013) Suspension of vacuum freez dried SNP's: influence of NaCl on their rheological properties. Carbohydr Polym 94:782–790

Sivamani S, Archana S, Santosh K, Sivarajasekar R, Parsad N (2018) Synthesis and characterisation of SNP's from cassava peel. J Bioresour Bioprod 3:161–165

Song S, Wang C, Pan Z, Wang X (2008) Preparation and characterization of amphiphilic starch nanocrystals. J Appl Polym Sci 107:418–422

Subaric D, Babic J, Lalic A, Ackar D, Kopjar M (2011) Isolation and characterisation of starch from different barley and oat varieties. Czech J Food Sci 29:354–360

Surendra Babu A, Parimalavalli R, Gaur Rudra S (2015) Effect of citric acid concentration and hydrolysis time on physicochemical properties of sweet potato starches. Int J Biol Macromol 80:557–565

Wei B, Xu X, Jin Z, Tian Y (2014) Surface chemical composition and diospersity of starch nanocrystals formed by sulfuric acid and hydrochloric acid hydrolysis. PLoS One 9:e86024

Xu C, Chen C, Wu D (2018) The SNC's filled biodegradable poly (ε-caprolactone) composite membrane with highly improved properties. Carbohydr Polym 182:115–122

Zambelli RA, Théóphilo Galvão AMM, de Mendonça LG, de Souza Leão MV, Carneiro SV, Silva Lima AC, Lemos Melo CA (2018) Effect of different levels of acetic, citric and lactic cassava starch modification on physical, rheological, microstructural properties. Food Sci Technol Res 24:747–754